JOURNAL OF COMPUTATIONAL PHYSICS 76, 414–425 (1988)

A Discrete Method for Anisotropic Angular Sampling in Monte Carlo Simulations

DOUGLAS R. WYMAN AND MICHAEL S. PATTERSON

Medical Physics Department, Hamilton Regional Cancer Centre, 711 Concession Street, Hamilton, Ontario, Canada L8V 1C3

Received January 30, 1987; revised April 30, 1987

A discrete method is presented for sampling anisotropic angular scattering distributions in Monte Carlo simulations. Derived from fundamental transport considerations, this method is based on equating the moments of a given distribution with those of a discrete distribution consisting of a sequence of Dirac delta spikes. The discrete method is slightly faster and, for a given scoring accuracy, more flexible than the tabular sampling method. Tests indicate that accuracy better than 1% in calculated transmittances is generally obtainable using only 4 spikes, provided the single scattering albedo exceeds 0.7. Conditions are described under which this method can be applied to heterogeneous media. © 1988 Academic Press, Inc

INTRODUCTION

The simulation of particle transport using the Monte Carlo method is well established and remains an area of active scientific application and research. Common applications involve the transport simulation of neutrons [1, 2], photons [1, 3, 4] and charged particles [3]. A practical summary of Monte Carlo simulation is given in the book by Carter and Cashwell [1].

In the biological sciences most simulations are designed to either estimate the absorption of photon energy in human tissues [4, 5] or simulate an imaging procedure [6]. By scoring reflectance or transmittance [7], fundamental interaction parameters can also be estimated.

The basic premise of Monte Carlo simulation is that complex particle–matter interactions can be treated as stochastic processes, and a single interaction can thus be simulated by random sampling from appropriate probability density functions. Accordingly, a great deal of effort has focused on developing mathematical techniques to reduce computation time by reducing the variance in scored quantities. The two classes of techniques commonly employed in variance reduction are biasing, denoting the sampling from altered probability density functions, and alterations of the scoring procedure. Frequently used biasing techniques are splitting and roulette [1], the exponential transform [8, 9], and biasing either the source or the angular scattering distribution [10, 11].

0021-9991/88 $3.00

For simulations involving highly anisotropic scattering, the scoring accuracy is often limited by the angular sampling procedure. A usual procedure is to fit the angular scattering probability density function (PDF) to an analytic function for which a known sampling procedure exists, usually based on sampling the uniform PDF [12].

Another useful approach is to approximate the angular scattering PDF by a sequence of spline functions. An intrinsically fast angular sampling method involves using a single sample of a uniform random variate to directly index a tabulated version of the angular scattering PDF. While conceptually simple, this and other "table look-up" methods are inconvenient for simulations where the angular scattering PDF is a parameter to be varied.

In this paper we derive, based on fundamental transport considerations, a discrete angular sampling method in which a given angular scattering PDF is replaced by a discrete PDF. The method should be useful for all neutral particle simulations and particularly those involving highly anisotropic scattering.

METHOD

The single energy group neutral particle transport equation, to be solved for the angular flux, ψ, or its various functionals, can be written using conventional notation [13] as

$$\frac{1}{v}\frac{\partial \psi}{\partial t} + \boldsymbol{\Omega}\cdot\nabla\psi + \Sigma_t(\mathbf{r})\,\psi(\mathbf{r},\boldsymbol{\Omega},t) - s(\mathbf{r},\boldsymbol{\Omega},t) = \int_{4\pi}\psi(\mathbf{r},\boldsymbol{\Omega}',t)\,\Sigma_s(\mathbf{r},\boldsymbol{\Omega}'\to\boldsymbol{\Omega})\,d\boldsymbol{\Omega}'. \quad (1)$$

The differential scattering cross-section, $\Sigma_s(\mathbf{r},\boldsymbol{\Omega}'\to\boldsymbol{\Omega})$, can also be written as a product of the total scattering cross-section, $\Sigma_s(\mathbf{r})$, and an angular scattering PDF $f(\mathbf{r},\boldsymbol{\Omega}'\to\boldsymbol{\Omega})$, so that the right-hand side of Eq. (1) becomes

$$\text{RHS} = \Sigma_s(\mathbf{r})\int_{4\pi}\psi(\mathbf{r},\boldsymbol{\Omega}',t)\,f(\mathbf{r},\boldsymbol{\Omega}'\to\boldsymbol{\Omega})\,d\boldsymbol{\Omega}'. \quad (2)$$

For randomly oriented scattering centres, $f(\mathbf{r},\boldsymbol{\Omega}'\to\boldsymbol{\Omega})$ is a function of the scattering angle, defined as the angle between the incident direction, $\boldsymbol{\Omega}'$, and exit direction, $\boldsymbol{\Omega}$. Denoting the cosine of this angle by μ_0, Eq. (2) can be rewritten as

$$\text{RHS} = \Sigma_s(\mathbf{r})\int_{4\pi}\psi(\mathbf{r},\boldsymbol{\Omega}',t)\frac{f(\mathbf{r},\mu_0)}{2\pi}\,d\boldsymbol{\Omega}', \quad (3)$$

where $f(\mathbf{r},\mu_0)$ is the PDF for μ_0. Note that for a given μ_0 there exists a continuum of azimuthal scattering angles between 0 and 2π.

A usual method of solving the transport equation, Eq. (1), involves expanding $f(\mathbf{r},\mu_0)$ using a complete polynomial set. While any complete set would work here,

the orthogonality property of the Legendre polynomials [14], $P_j(\mu_0)$, renders convenient the following expansion:

$$f(\mathbf{r}, \mu_0) = \sum_{j=0}^{\infty} \left(\frac{2j+1}{2}\right) f_j P_j(\mu_0). \tag{4}$$

For notational convenience, the $\mathbf{r}$ dependence of f_j is suppressed. By orthogonality, the expansion coefficients are calculated using

$$f_j = \int_{-1}^{1} f(\mathbf{r}, \mu_0)\, P_j(\mu_0)\, d\mu_0. \tag{5}$$

Substituting Eq. (4) into Eq. (3) yields

$$\text{RHS} = \sum_{j=0}^{\infty} f_j\, g_j(\mathbf{r}, \boldsymbol{\Omega}, t) \tag{6}$$

with

$$g_j(\mathbf{r}, \boldsymbol{\Omega}, t) = \left(\frac{2j+1}{4\pi}\right) \Sigma_s(\mathbf{r}) \int_{4\pi} \psi(\mathbf{r}, \boldsymbol{\Omega}', t)\, P_j(\mu_0)\, d\boldsymbol{\Omega}'. \tag{7}$$

From Eq. (6) it is clear that any angular scattering PDF, $f^*(\mathbf{r}, \mu_0)$, with its Legendre expansion coefficients given by f_j^*, yields the same solution to the transport equation as does $f(\mathbf{r}, \mu_0)$, if and only if

$$\sum_{j=0}^{\infty} g_j(\mathbf{r}, \boldsymbol{\Omega}, t)[f_j - f_j^*] = 0. \tag{8}$$

Since Eq. (8) must hold for all $\mathbf{r}, \boldsymbol{\Omega}, t$, it follows that $f^*(\mathbf{r}, \mu_0)$ is equivalent to $f(\mathbf{r}, \mu_0)$, according to Eq. (8), if and only if

$$f_j^* = f_j \qquad \text{or} \qquad g_j(\mathbf{r}, \boldsymbol{\Omega}, t) = 0, \qquad j \geqslant 0. \tag{9}$$

Note that Eq. (9) always holds for $j = 0$ since both $f(\mathbf{r}, \mu_0)$ and $f^*(\mathbf{r}, \mu_0)$ are PDFs. Equation (9) is easily understood by reference to the following three cases, in which the scalar flux, $\phi(\mathbf{r}, t)$, is the angular flux integrated over all solid angles:

(i) The angular flux is isotropic and can thus be written as

$$\psi(\mathbf{r}, \boldsymbol{\Omega}, t) = \phi(\mathbf{r}, t)/4\pi. \tag{10}$$

Here, $g_j = 0$ for $j > 0$ and any $f^*(\mathbf{r}, \mu_0)$ is equivalent to $f(\mathbf{r}, \mu_0)$.

(ii) The angular flux is linearly (1st-order) anisotropic and can thus be written as

$$\psi(\mathbf{r}, \boldsymbol{\Omega}, t) = (\phi(\mathbf{r}, t) + \boldsymbol{\Omega} \cdot \boldsymbol{\psi}_1(\mathbf{r}, t))/4\pi. \tag{11}$$

It can be shown here, using the addition theorem [14], that $g_j = 0$ for $j > 1$. Equivalence, Eq. (9), therefore demands $f_1^* = f_1$, i.e., equal average cosines of the scattering angle.

(iii) The angular flux is Nth order anisotropic and can thus be written using conventional spherical harmonics [14] as

$$\psi(\mathbf{r}, \mathbf{\Omega}, t) = \sum_{n=0}^{N} \sum_{m=-n}^{n} a_{mn}(\mathbf{r}, t)\, Y_n^m(\theta, \xi). \tag{12}$$

Using both the addition theorem and orthogonality properties [14], it can be shown that $g_j = 0$ for $j > N$. Equivalence, Eq. (9), therefore demands

$$f_j^* = f_j, \qquad j = 0, ..., N. \tag{13}$$

Given the definition of f_j in Eq. (5), Eq. (13) implies that scattering equivalence for an Nth order anisotropic flux also demands equal moments of the scattering PDF, as

$$\mu_0^{(j)*} = \mu_0^{(j)}, \qquad j = 0, ..., N, \tag{14}$$

where

$$\mu_0^{(j)} = \int_{-1}^{1} \mu_0^j\, f(\mathbf{r}, \mu_0)\, d\mu_0. \tag{15}$$

The above transport-based derivation formalizes the notion that the similarity of two functions can be measured by the similarity of their moments. While the above theory may be of some analytic utility, its application to Monte Carlo particle transport simulations is clear. For cases where the scattering is highly anisotropic or angularly irregular, it would be faster to sample a simpler, but approximately equivalent, angular scattering distribution than to sample $f(\mathbf{r}, \mu_0)$ directly. Similarity relations have been previously described [15]. Unfortunately, these relations are derived for homogeneous slab geometry and are not valid near internal boundaries of multi-region geometries where the angular flux is highly anisotropic.

Sampling of the scattering angle in Monte Carlo calculations is fastest and easiest when $\mu_0 = \pm 1$ since, for these limiting cases, no additional sampling is required for the azimuthal scattering angle. For all other values of μ_0, the azimuthal angle is always sampled uniformly. Isotropic scattering is easily simulated since both μ_0 and the azimuthal scattering angle can be sampled uniformly relative to any Cartesian coordinate system. In the general case, however, the fastest conceivable sampling would involve selecting a fixed forward angle, μ_0^*, corresponding to the PDF

$$f^*(\mathbf{r}, \mu_0) = \delta(\mu_0 - \mu_0^*(\mathbf{r})), \tag{16}$$

where δ denotes the Dirac delta distribution. For this PDF, the equal moments requirement in Eq. (14), with $N=1$, fixes μ_0^* at $\bar{\mu}_0$, the average value of μ_0. Since matching higher moments ($N>1$) overdetermines $f^*(\mathbf{r}, \mu_0)$, the practice of always selecting $\bar{\mu}_0$ for the value of μ_0 is exact only in regions where the flux is linearly anisotropic, defined as the diffusion regime.

The simple and fast sampling method represented by Eq. (16) is easily extended to admit a higher order of flux anisotropy. In general, the equivalent scattering PDF consists of multiple Dirac delta spikes and is of the form

$$f^*(\mathbf{r}, \mu_0) = \sum_{k=1}^{N} a_k \delta(\mu_0 - \mu_{k0}^*). \tag{17}$$

The equal moments requirement in Eq. (14), using the first N equations, results in the following system of N equations in $2N$ unknowns, namely a_k and μ_{k0}^*:

$$\sum_{k=1}^{N} a_k (\mu_{k0}^*)^j = \mu_0^{(j)}, \qquad j=0, \ldots, N-1. \tag{18}$$

Equation (18) can be converted to an $N \times N$ nonlinear system by specifying that all spikes have the same amplitude, and by adding an equation for $j=N$. Unfortunately, the solutions for μ_{k0}^* frequently exceed 1.0 and are therefore unphysical. Fortunately, Eq. (18) can also be converted to an $N \times N$ linear system by prespecifying the spike locations, μ_{k0}^* and then solving for the spike amplitudes, a_k. Logical choices for spike locations are at $\mu_{k0}^* = 0$, 1, $\bar{\mu}_0$, $-\bar{\mu}_0$, since each of these values either simplifies the $N \times N$ system or renders sampling of the azimuthal angle unnecessary. In order to ensure solutions of a_k between 0 and 1, it is necessary to select spike locations on either side of $\bar{\mu}_0$.

For example, restricting the discussion to forward peaked scattering, the first five $N \times N$ systems employ the spike locations listed in Table I. The 5×5 system is the most accurate of these, and is given by:

$$\left[\begin{array}{ccccc|c} 1 & 1 & 1 & 1 & 1 & 1 \\ \bar{\mu}_0 & -\bar{\mu}_0 & -1 & 0 & 1 & \bar{\mu}_0 \\ \bar{\mu}_0^2 & \bar{\mu}_0^2 & 1 & 0 & 1 & \mu_0^{(2)} \\ \bar{\mu}_0^3 & -\bar{\mu}_0^3 & -1 & 0 & 1 & \mu_0^{(3)} \\ \bar{\mu}_0^4 & \bar{\mu}_0^4 & 1 & 0 & 1 & \mu_0^{(4)} \end{array}\right]. \tag{19}$$

Analytic solutions to these linear systems are easily found. Only those solutions for which $0 \leqslant a_k \leqslant 1$ are acceptable for Monte Carlo sampling. Solutions to the 1×1 and 2×2 systems always satisfy this range criterion. Solutions to the 3×3 system, however, satisfy the range criterion if and only if the first and second moments obey the inequality

$$\bar{\mu}_0^2 \leqslant \mu_0^{(2)} \leqslant \bar{\mu}_0. \tag{20}$$

TABLE I

Spike Locations for Discrete Angular Scattering PDF That Is Equivalent to a Continuous PDF with Average Cosine $\bar{\mu}_0$

N	Spike locations
1	$\bar{\mu}_0$
2	$(0, 1)$
3	$(\bar{\mu}_0, 0, 1)$
4	$(\bar{\mu}_0, 0, \pm 1)$
5	$(\pm\bar{\mu}_0, 0, \pm 1)$

Equation (20) generally holds for highly forward peaked scattering. For example, the Henyey–Greenstein angular scattering function [15], discussed in the next section, obeys Eq. (20) for values of $\bar{\mu}_0 > 0.5$. Inequalities similar to Eq. (20) can also be derived for the 4×4 and 5×5 system. For example, any Henyey–Greenstein function with $\bar{\mu}_0 > 0$ results in acceptable solutions to the 4×4 system, corresponding to the 4-spike PDF. The 5×5 system is much more sensitive and frequently yields negative a_k values. In these instances the more robust 4-spike function should be used.

The multiple spike angular scattering PDF should not be confused with discrete ordinate methods [13], in which the angular flux is represented by its values at a discrete set of angles. It should be emphasized that the spike configurations in Table I are just a few of the many possible. Generally, the spike locations or amplitudes or both may be left variable in an attempt to match as many moments as possible. The question of optimal spike PDF selection remains unresolved. The spike configurations in Table I, however, have the desirable properties that they lead to easily solvable linear systems with easily determined ranges of applicability, as described above. We have found that leaving spike locations variable results in nonlinear equation systems with solutions for spike locations that unpredictably fall outside the physical range $(-1, 1)$.

Results and Discussion

The above method for replacing a given angular scattering PDF by a PDF consisting of a sequence of spikes of different amplitudes was tested in a Monte Carlo code developed at our institution. The code was developed for heterogeneous media in accordance with the general principles of Monte Carlo simulation, including non-absorption weighting and exponential biasing [1] and was verified prior to testing the above angular sampling method. All exact solutions were obtained from standard tables [15] which were calculated using the doubling method [16].

Additional verification of the Monte Carlo code and testing of the sampling method were provided by having 4th- and 5th-order results (4 spikes) that approached the exact solutions. Results indicating the accuracy of the sampling method are provided in Fig. 1, for which the relative error in calculated transmittance is plotted as a function of both the order of the equivalent spike PDF and $\bar{\mu}_0$. The exact angular scattering PDF employed is a Henyey–Greenstein function [15], being a smooth PDF with a single parameter, $\bar{\mu}_0$, with the useful property that f_j is simply $\bar{\mu}_0^j$, and with the following functional form:

$$f_{HG}(\mu_0) = 2(1-\bar{\mu}_0^2)(1+\bar{\mu}_0^2-2\bar{\mu}_0\mu_0)^{-3/2}. \tag{21}$$

The simulations were done for normal incidence on a homogeneous test slab of thickness 8 mean free paths (mfp), characterized by the single scattering albedo $\Sigma_s/\Sigma_t = 0.9$. Approximately 125,000 particle histories were simulated for each plotted point, sufficient to reduce the statistical error to less than one-fifth the relative transmittance error in all cases except those where the relative transmittance error is less than 1%.

As expected, the accuracy of the method increases with N, the number of spikes employed, corresponding to the number of moments matched, Eq. (18). The discrete PDF with $N = 5$ is only slightly more accurate than with $N = 4$ and could only be used with $\bar{\mu}_0 = 0.875$. Since the variation in μ_0 decreases as scattering becomes increasingly foward peaked, the observed increase in accuracy is also expected. As $\bar{\mu}_0$ approaches 1.0, the spike amplitude at $\bar{\mu}_0$ approaches 1.0. In general, accuracy

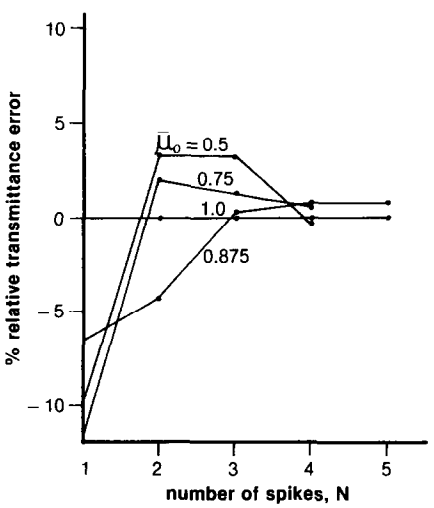

FIG. 1. Relative transmittance error when a Henyey–Greenstein angular scattering PDF is replaced by a discrete PDF using N spikes, for normal incidence on a homogeneous test slab of thickness 8 mean free paths with $\Sigma_s/\Sigma_t = 0.9$. $N = 5$ can only be employed when $\bar{\mu}_0 = 0.875$. The correct transmittance values are 0.0544, 0.1306, 0.2335, and 0.4493 for $\bar{\mu}_0 = 0.5$, 0.75, 0.875, and 1.0, respectively.

greater than 1% in the transmittance is obtainable with this method, and 4 spikes is the preferred discrete function.

The method was also tested for the case of normal incidence on a homogeneous slab of thickness 8 mfp, with the albedo, α, varied between 0.4 and 1.0, and with $\bar{\mu}_0 = 0.875$. The results are displayed as the two lower curves in Fig. 2. For an albedo greater than 0.7, accuracy to within 1% is obtainable. For an albedo less than 0.6, however, the accuracy of the method decreases rapidly. This decrease is expected, since decreasing the albedo increases the flux anisotropy. Accuracy of the method could not be assessed when the albedo is less than 0.4 since in this range the published exact solutions [15] contain at most one significant digit.

A third test of the method involved simulating normal incidence on a homogeneous slab with variable thickness, albedo of 0.9, and $\bar{\mu}_0 = 0.875$. The results are displayed as the upper curve in Fig. 2, from which it is evident that the method is relatively insensitive to slab thickness. While the calculated transmittance is accurate to within 1% for slabs as thin as 0.5 mfp, the angular flux for these thin slabs would be very inaccurate. The method should thus work for heterogeneous media, provided the heterogeneities are spaced at least a few mfp apart so that the angular flux incident on a given region is correct. Accordingly, testing involved

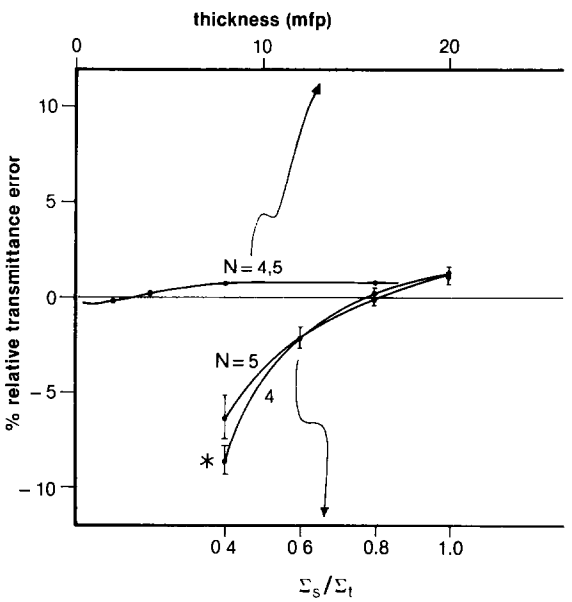

FIG 2. Relative transmittance error when a Henyey–Greenstein angular scattering PDF with $\bar{\mu}_0 = 0.875$ is replaced by a discrete PDF using N spikes. Error bars indicate statistical uncertainty: upper curve, variable thickness and $\Sigma_s/\Sigma_t = 0.9$; lower curves, thickness of 8 mfp and Σ_s/Σ_t is variable; *, $\pm 1\%$ additional error in "correct" value.

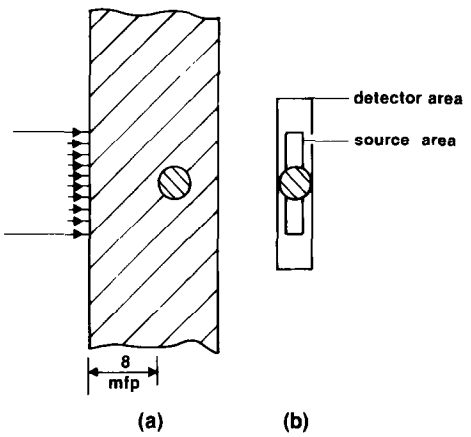

FIG. 3. Rectangular beam normally incident on a homogeneous infinite slab of thickness 15 mfp, albedo 0.95, and $\bar{\mu}_0 = 0.617$. Inside the slab is a homogeneous sphere of diameter 4 slab mfp, albedo 0.90, $\bar{\mu}_0 = 0.5$, and Σ_t one-fourth that in the slab: (a) side view; (b) front view illustrating source and detection geometries

simulating imaging of the homogeneous slab with an embedded sphere, shown in Fig. 3.

An image of the sphere is indicated by the transmission ratios in Fig. 4. The image is blurred since scattering is not highly forward peaked. Spline PDFs were used as the actual angular scattering PDFs for both the sphere and slab regions so that, within statistical error, the spline curve is accurate. The corresponding ratios obtained using the spline and discrete PDFs all agree within statistical error,

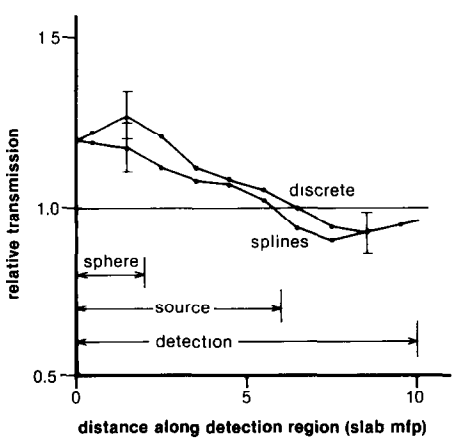

FIG. 4. Ratio of transmission with sphere to transmission without sphere in the slab of Fig. 3, using both the discrete and spline angular sampling methods. Error bars indicate the statistical uncertainty in transmission values after smoothing (1:2:1) the original histogram data.

although the discrete method ratios are consistently the highest. This bias is greatest near the sphere image and suggests that the discrete method slightly overestimates transmission.

If the same sphere is embedded in a thinner but otherwise identical slab, the relative overestimation obtained using the discrete PDF increases. For thicker slabs the overestimation decreases. The transmission overestimation only occurs near the sphere image and arises from repeated scattering at $\mu_0 = 1.0$, of part of the collimated beam. The resulting extra collimated beam tends to project directly through the relatively translucent sphere, resulting in significant overestimation of transmission if the sphere is too close to the slab entrance face.

In general, a minimum distance exists between material boundaries that enables the discrete PDF method to reproduce the angular flux incident on these boundaries to an accuracy limited by flux anisotropy. This minimum distance, $d_{\min}$, should be largest for the case of normal incidence, such as that in Fig. 3. A general value for $d_{\min}$ can therefore be calculated by requiring that at an internal and normal displacement of $d_{\min}$, the collimated beam is a small fraction of the transmittance, T_{homo}, for a homogeneous slab of thickness $d_{\min}$. Specifying the small fraction as 1%, this requirement can be written from considerations of exponential attenuation as

$$\exp[-d_{\min}(\Sigma_a + \Sigma_s(1 - a_N))] < T_{\text{homo}}/100, \tag{22}$$

where a_N is the amplitude of the spike at $\mu_0 = 1$. This leads to

$$d_{\min} > \frac{\ln(T_{\text{homo}}/100)}{\alpha a_N - 1} \text{ mfp}. \tag{23}$$

For the configuration in Fig. 3, $d_{\min}$ is approximately 9 mfp. Since the sphere is only 8 mfp from the slab entrance face, the observed slight overestimation in transmission, Fig. 4, is expected.

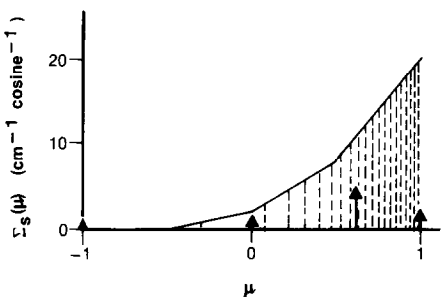

FIG 5 Test spline function for $\Sigma_s(\mu)$ illustrating tabular approximation based on equal probability spacing (---), and discrete approximation based on 4 spikes of relative heights as shown (↑). Here $\bar{\mu}_0 = 0.617$.

TABLE II

Comparison of Three Angular Sampling Methods for the Spline Angular Scattering PDF Given in Fig 5, and for Which the Spline Method is Exact, Apart from the Stated Statistical Error

Sampling method	Time	Transmittance
Tabular (20 entries)	1.0	$0.0721 \pm 0.5\%$
Splines	1.09	$0.0742 \pm 1.0\%$ (exact)
Discrete	0.87	$0.0744 \pm 0.5\%$

Note. Values were obtained for normal incidence on the test slab with $\bar{\mu}_0 = 0.617$. Computation time is normalized to 1.0 for the tabular method.

To test the speed of the discrete angular sampling method, simulations were conducted on the test slab, with the spline PDF shown in Fig. 5, and for which the spline method is therefore exact. The discrete (4 spikes) and tabular (20 entries) equivalent PDFs were sampled in separate simulations and are also shown in Fig. 5. A comparison of the relative computation times and accuracies of these three angular sampling methods is given in Table II. Discrete angular sampling is fastest irrespective of the number of table entries or splines used since it renders computation of direction matrices unnecessary for scattering with $\mu_0 = 1$. The difference in computation time between the discrete and tabular methods is approximately proportional to a_N and independent of table size. Additionally, more than 20 table entries are necessary to achieve the accuracy obtained with 4 spikes.

SUMMARY

A discrete angular sampling method has been derived based on matching the first N moments of a given continuous angular scattering PDF with the first N moments of a discrete PDF consisting of a sequence of N Dirac delta spikes. The accuracy of Monte Carlo simulations using the discrete method increases with N. If a single spike is used, the simulation is exact in the diffusion regime, characterized by linear flux anisotropy. When $N > 1$ spikes are used, the simulation is exact in regions where the flux anisotropy is of order $N - 1$. Statistical errors aside, computed transmittances for homogeneous slabs with $N = 4$ are generally accurate to within 1%, provided the single scattering albedo exceeds 0.7. For simulations in heterogeneous media, an estimable minimum separation of material boundaries exists that preserves the inherent accuracy of this method.

The discrete angular sampling method works best for highly forward peaked scattering with a high albedo. The choice of spike locations is arbitrary, although not all sets of locations generate positive spike amplitudes. The $N = 4$ set suggested in this paper reliably generates positive amplitudes for all forward scattering PDFs we have encountered.

In Monte Carlo simulations, the discrete method and tabular method require comparable computational effort, since each procedure requires as input a discrete representation of a continuous PDF and thereupon performs basic numerical integration. The discrete method is, however, slightly faster than the tabular method and more flexible, since far fewer spikes than table entries are required for each region in a heterogeneous medium.

REFERENCES

1. L. L. CARTER AND E. D. CASHWELL, *Particle-Transport Simulation with the Monte Carlo Method* (U.S. Energy Research and Development Administration, 1975).
2. SPANIER AND E. M GELBARD, *Monte Carlo Principles and Neutron Transport Problems* (Addison-Wesley, London, 1969).
3. W R NELSON, H HIRAYAMA, AND D. W. O. ROGERS, Stanford Linear Accelerator Center Report, SLAC-265, 1985 (unpublished).
4. H.-P. CHAN AND K. DOI, *Med. Phys.* **11**, 480 (1984).
5. B C WILSON AND G. ADAM, *Med. Phys.* **10**, 824 (1983).
6. J. M. MAAREK, G. JARRY, J CROWE, M. H. BUI, AND D. LAURENT, *Med. Biol. Eng. Comput.* **24**, 407 (1986)
7. P A. WILKSCH, F JACKA, AND A J BLAKE, in *Porphyrin Localization and Treatment of Tumors* (A. R. Liss, New York, 1984), p. 149.
8. L. B. LEVITT, *Nucl. Sci. Eng.* **31**, 500 (1968).
9. M. LEIMDORFER, *Nukleonik* **6**, 58 (1964).
10. C. E. BURGART AND F. N STEVENS, *Nucl. Sci. Eng.* **42**, 306 (1970)
11. J. M LANORE, *Nucl. Sci. Eng.* **45**, 66 (1971).
12. R A J. GROENHUIS, H. A. FERWERDA, AND J. J. TEN BOSCH, *Appl Opt.* **22**, 2456 (1983).
13. J. J. DUDERSTADT AND L. J HAMILTON, *Nuclear Reactor Analysis* (Wiley, New York, 1976).
14. G. B. ARFKEN, *Mathematical Methods for Physicists* (Academic Press, New York, 1970).
15. H. C. VAN DE HULST, *Multiple Light Scattering* (Academic Press, New York, 1980), Vol. 2.
16. H. C. VAN DE HULST AND K GROSSMAN, in *The Atmospheres of Venus and Mars*, edited by J. C. Brandt (Gordon & Breach, New York, 1968).